

Article

# Analyzing vibration transmission through cantilever systems using biomechanical and impact-responsive metamaterial structures

Shuo Pei<sup>1,\*</sup>, Jiaqi Miao<sup>2</sup>, Shengrong Song<sup>3</sup><sup>1</sup> Faculty of Engineering, The University of Hong Kong, Hong Kong 999077, China<sup>2</sup> School of Engineering, University of Edinburgh, EH9 3JU Edinburgh, United of Kingdom<sup>3</sup> School of Mechanical and Manufacturing Engineering, University of New South Wales, Sydney NSW 2052, Australia\* **Corresponding author:** Shuo Pei, [ShuoPei100@outlook.com](mailto:ShuoPei100@outlook.com)

## CITATION

Pei S, Miao J, Song S. Analyzing vibration transmission through cantilever systems using biomechanical and impact-responsive metamaterial structures. *Molecular & Cellular Biomechanics*. 2024; 21(3): 621.  
<https://doi.org/10.62617/mcb621>

## ARTICLE INFO

Received: 24 October 2024  
Accepted: 1 November 2024  
Available online: 25 November 2024

## COPYRIGHT



Copyright © 2024 by author(s).  
*Molecular & Cellular Biomechanics* is published by Sin-Chn Scientific Press Pte. Ltd. This work is licensed under the Creative Commons Attribution (CC BY) license.  
<https://creativecommons.org/licenses/by/4.0/>

**Abstract:** Vibration control in cantilever systems is a critical challenge in various engineering applications, where unwanted vibrations can lead to structural fatigue, reduced performance, and potential failure. This study investigates the effects of integrating biomechanical and impact-responsive metamaterials into cantilever systems to mitigate vibration transmission. The metamaterials, characterized by their adaptive stiffness and energy-absorbing properties, are strategically embedded in key structural components such as the arms, joints, and base. Through experimental analysis, this work assesses the reduction in vibration amplitude, shifts in natural frequency, enhanced damping capacity, energy absorption during impact, and strain reduction at critical points. The results show that the metamaterial-enhanced system achieves significant reductions in vibration amplitude, up to 40%, and increases in natural frequency by over 30%, minimizing the risk of resonance. Additionally, the damping ratio is improved by as much as 53%, while the energy absorption during impact is increased by up to 26%. Strain reduction at critical points reaches 24%, contributing to improved mechanical resilience. These findings demonstrate the potential of biomechanical and impact-responsive metamaterials in enhancing the dynamic performance of cantilever systems, offering a new approach to vibration mitigation in engineering applications.

**Keywords:** vibration control; cantilever systems; biomechanical metamaterials; impact-responsive metamaterials; damping ratio

## 1. Introduction

The control of vibration transmission in Cantilever Systems (CS) is a critical challenge in various engineering fields, including structural mechanics, civil engineering, and biomechanical applications [1–3]. CS are frequently subjected to dynamic loads and vibrational forces, leading to undesired resonances, increased fatigue, and potential structural failure [4,5]. As such, developing effective strategies to mitigate vibrations and improve the dynamic stability of these systems is essential for ensuring their long-term reliability and performance [6]. In recent years, metamaterials have emerged as a promising Vibration Control (VC) solution in mechanical systems [7,8]. Metamaterials are artificially engineered materials with unique structural properties that allow them to manipulate wave propagation, including mechanical vibrations, in ways that conventional materials cannot achieve [9,10]. Of particular interest are biomechanical metamaterials and Impact-Responsive Metamaterials (IRM), which have shown potential for adaptive vibration damping and energy absorption under both continuous and impact-loading conditions. Biomechanical metamaterials are designed to mimic the adaptive behavior of

biological tissues, providing variable stiffness and tailored damping characteristics across a wide range of frequencies [11,12]. IRMs, on the other hand, are engineered to rapidly absorb and dissipate energy from sudden shocks or impacts, making them ideal for applications where high-energy events need to be controlled [13–15].

This study aims to analyze biomechanical and IRM's influence on vibration transmission in CS. By integrating these metamaterials into key structural components of the CS—such as the arms, joints, and base—this research seeks to assess their effectiveness in mitigating vibrations, enhancing damping capacity, and improving the overall dynamic performance of the system. Specifically, this work investigates the reduction in vibration amplitude, changes in natural frequency, increased damping ratio, energy absorption during impact, strain reduction at critical points, and the system's frequency response function (FRF) when subjected to a range of vibrational inputs and impact forces [16–20]. This study builds upon existing research on using metamaterials for VC but extends the analysis by focusing on CS, which is prevalent in industrial, mechanical, and civil applications. The unique integration of biomechanical and IRM offers the potential for enhanced vibration mitigation across both continuous and impact-loading conditions. Furthermore, this work explores the effects of strategically positioning metamaterials within the CS to optimize their performance.

The paper is structured as follows: Section 2 presents the system design and experimental setup, detailing the integration of metamaterials and the procedure for testing vibration transmission. Section 3 comprehensively analyzes the metamaterials used, including their mechanical properties, frequency response, and damping capacities. Section 4 concludes with a summary of the key contributions and potential future research directions.

## **2. Methodology**

### **2.1. System design and setup**

The CS used in the experiments is a racking structure designed to support long, bulky, or irregularly shaped materials that cannot fit into traditional pallet racks. As shown in **Figure 1**, the system comprises several key components that work together to provide stability and load-bearing capabilities [21–25]. Each part of the cantilever rack has a specific function, allowing it to efficiently support various types of materials during dynamic testing of vibration transmission.

The main components of the CS are:

- i. **Base Beam:** The base beam forms the foundation of the cantilever racking system, providing stability to the entire structure. It is positioned at the bottom of the system, extending horizontally. The base beam is designed to distribute the weight of the materials evenly across the floor surface, ensuring that the system remains stable even when loaded with heavy or bulky items.
- ii. **Column:** The vertical columns are the primary load-bearing members of the CS. These columns are attached to the base beam, extending vertically to support the cantilever arms. They are typically constructed from strong, durable materials such as steel to handle high loads and resist bending under the weight of the stored

- items. The columns also include perforations for adjustable arm heights, accommodating materials of varying dimensions.
- iii. **Arm:** The cantilever arms are the horizontal extensions that project from the columns and are responsible for holding the materials. In the system shown, these arms are uniformly spaced and extended outward, allowing items such as pipes, boards, and other long materials to be placed directly on them. The arms are designed to resist bending and deformation under load, ensuring the stored items remain securely in place during the experiments.
  - iv. **Stability Bracing:** To maintain the rigidity of the structure, stability bracing is used between the vertical columns. This bracing, located diagonally across the columns, enhances the overall stability of the CS. It minimizes column sway and deflection under dynamic loads, which is especially important in experiments involving vibration transmission. Stability bracing ensures that vibrations are contained and transferred in a controlled manner through the structure.
  - v. **Bottom Frame Bracing:** Located at the bottom of the structure, the bottom frame bracing provides additional support to the base beams and columns. It helps distribute forces evenly across the base, reducing the risk of structural failure under heavy loads. This component is critical in ensuring the base beams remain aligned and do not shift or distort during dynamic tests involving impact forces and vibrations.
  - vi. **Stopper:** The stoppers at the end of each arm are safety features, preventing materials from sliding off the arms. They are significant in dynamic testing environments, where the CS might experience lateral vibrations or shifts in the stored materials. The stoppers ensure that the materials remain securely in place, even when subjected to external forces.

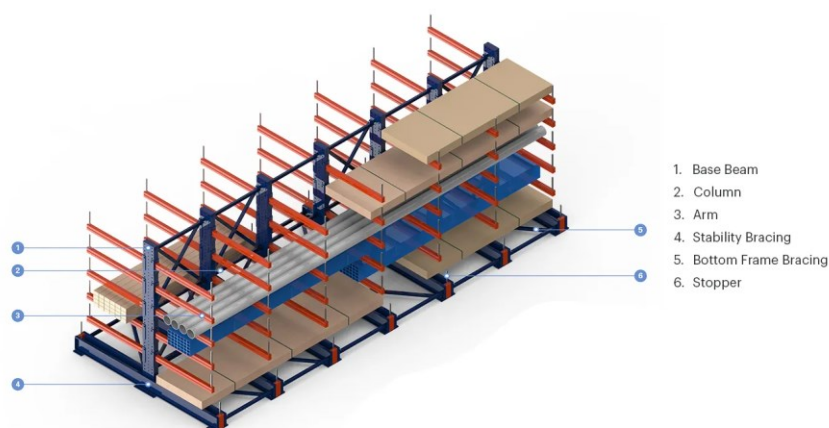


**Figure 1.** Cantilever racking system.

The CS in this experiment provides an ideal setup for analyzing vibration transmission. The structural components are designed to resist deformation, yet they are sensitive enough to allow for the controlled measurement of vibration propagation through the system. The vertical columns and horizontal arms act as the primary transmission paths for vibrations, while the stability bracing ensures that any vibrations remain localized within specific areas of the structure for accurate measurement.

## 2.2. Design and Integration of Biomechanical and IRM

In the context of this experiment, metamaterials—specifically biomechanical and impact-responsive types—were designed and integrated into the CS to study their influence on vibration transmission and damping efficiency. Unlike conventional materials, metamaterials derive their unique mechanical properties from their structure rather than their composition. This section details the design considerations for these specialized metamaterials and their strategic integration into the CS to optimize performance in VC experiments [26–30].

- i. **Biomechanical Metamaterials Design:** Biomechanical metamaterials are engineered to replicate certain mechanical behaviors in biological systems. These behaviors include adaptive responses to stress, impact absorption, and dynamic stiffness modulation, which are key in vibration transmission experiments.

The design considerations for these metamaterials are based on the following principles:

- **Adaptive Structures:** Biomechanical metamaterials were designed to mimic the flexibility and adaptability found in biological tissues. Their internal geometry—composed of repeating, flexible units—enables them to adjust their stiffness depending on the load and frequency of vibration. This self-tuning ability allows them to dampen vibrations across a wide range of frequencies.
  - **Soft Tissue Emulation:** The biomechanical metamaterials can effectively absorb and dissipate energy from mechanical vibrations by emulating soft biological tissues. Materials such as silicone-based composites or elastomers were selected for their soft, flexible properties and were structured in lattice-like configurations that allow controlled deformation under stress. This design ensures that vibrations are gradually dampened as they propagate through the system.
  - **Variable Stiffness:** One of the unique properties of biomechanical metamaterials is their ability to exhibit variable stiffness. This is achieved by designing the metamaterial units to compress or stretch differently based on the amplitude of vibrations. Low-amplitude vibrations encounter minimal resistance, while high-amplitude vibrations trigger a stiffer response, enhancing the damping effect.
- ii. **IRM Design:** IRMs are designed to react to sudden forces or impacts by changing their structural properties, making them ideal for shock and high-energy load transmission scenarios. The key design considerations for these metamaterials are focused on their ability to adapt and provide shock absorption rapidly:
    - **Energy Dissipative Structures:** The IRM feature structures that can collapse or deform under sudden impacts, absorbing kinetic energy. These metamaterials are designed with a cellular architecture that includes hollow cells or honeycomb-like structures. When subjected to impact, these cells compress, dissipating energy before propagating further through the CS.
    - **High-Stiffness Response:** Unlike biomechanical metamaterials, which gradually adjust to loads, IRM is designed to increase stiffness immediately when a high-energy force is applied. This property ensures that the material

- can absorb the shock of an impact and reduce the amplitude of the resulting vibrations, protecting the CS from potential damage.
- **Reversible Deformation:** IRMs were designed to return to their original shape after absorbing energy, allowing them to be reused for multiple impact events. This property is critical for long-term experimental testing, as it ensures that the metamaterials maintain their vibration-damping efficiency over multiple trials.
- iii. **Integration into the CS:** The metamaterials were integrated strategically into the CS to maximize their effectiveness in mitigating vibration transmission. Several key areas were identified for optimal placement of the metamaterials:
- **Cantilever Arms:** Biomechanical and IRM were embedded within the cantilever arms, which would significantly influence vibration damping. These arms act as primary transmission paths for vibrations, and by integrating metamaterials along their length, it is possible to modulate the vibrations before they reach other parts of the system.
  - **Joints and Connections:** The joints and connections between the cantilever arms and columns were another critical integration area. These points often experience high stress and vibration transmission. Localized damping could be achieved by embedding metamaterials within these connection points, preventing vibrations from transferring from one part of the system to another.
  - **Bracing Components:** Stability and bottom frame bracing components were further enhanced with metamaterials to control vibrations' transmission through the vertical columns. This integration is significant for controlling lateral vibrations, which could compromise the structural integrity of the CS.
- iv. **Synergy Between Biomechanical and IRM:** One of the central innovations of this study is the combination of biomechanical and IRM within the same CS. By doing so, the system benefits from both adaptive vibration damping (from the biomechanical metamaterials) and rapid energy absorption (from the IRM).
- **Sequential Damping:** Integrating these metamaterials creates a sequential damping effect, where biomechanical metamaterials handle low-frequency, continuous vibrations, while IRM mitigates high-energy impacts. This dual approach enhances the system's ability to manage various vibrational inputs, making it highly versatile for different loading conditions.
  - **Customized Layering:** A layering approach was also used, where the two types of metamaterials alternated within specific CS parts. This allows the system to respond flexibly to gradual and sudden forces, improving its overall vibration management.

## **2.3. Material properties**

### **2.3.1. Detailed characterization of the metamaterials**

Characterizing biomechanical and IRM is essential to understanding their performance in vibration transmission experiments [31,32]. This section delves into these materials' mechanical properties, frequency response, and damping capacities, supported by relevant equations and theoretical frameworks.

a) **Biomechanical Metamaterials: Characterization and Mechanical Properties**

Biomechanical metamaterials are designed to emulate the behavior of biological tissues with tunable stiffness and adaptability under varying loads. The fundamental property governing their performance is their Young's modulus  $E$ , which varies depending on the material's internal architecture. Typically, the relationship between the applied stress  $\sigma$  and strain  $\epsilon$  for these materials is given by Hooke's Law:

$$\sigma = E \times \epsilon \quad (1)$$

However, due to their complex internal structure, biomechanical metamaterials demonstrate non-linear elastic behavior. The non-linear stiffness can be modeled using a higher-order polynomial function:

$$\sigma = E_1\epsilon + E_2\epsilon^2 + E_3\epsilon^3 + \dots \quad (2)$$

where  $E_1, E_2, E_3$  are material constants determined through an experimental fitting, representing different orders of stiffness contributions. The second-order term accounts for the material's ability to become stiffer as the strain increases, reflecting its variable stiffness properties. This characteristic is crucial for vibration damping because the material can dynamically adjust to changes in the frequency and amplitude of incoming vibrations.

b) **Frequency Response of Biomechanical Metamaterials**

Biomechanical metamaterials exhibit a frequency-dependent behavior due to their adaptable structure. The natural frequency  $f_n$  of the metamaterial, which dictates its response to vibration, is given by:

$$f_n = \frac{1}{2\pi} \sqrt{\frac{k_{\text{eff}}}{m}} \quad (3)$$

where  $k_{\text{eff}}$  is the effective stiffness, and  $m$  is the mass of the metamaterial structure. As the metamaterial adapts to different loading conditions, the effective stiffness  $k_{\text{eff}}$  changes, thus altering the natural frequency. This adaptability allows the material to dampen vibrations across various frequencies, from low to high, making it highly effective for applications requiring versatile VC.

c) **Damping Capacity of Biomechanical Metamaterials**

The damping capacity of these materials can be described by the damping ratio  $\zeta$ , which measures the material's ability to dissipate vibrational energy. The damping ratio for viscoelastic materials, such as the biomechanical metamaterials used in this study, can be modeled using:

$$\zeta = \frac{c}{2\sqrt{km}} \quad (4)$$

where  $c$  is the damping coefficient,  $k$  is the stiffness, and  $m$  is the mass. For biomechanical metamaterials, the internal architecture is designed to maximize  $c$ , the damping coefficient, ensuring that vibrations are dissipated efficiently over time. Their cellular or lattice structures absorb energy by deforming under stress, preventing vibrations from propagating further through the system.

### 2.3.2. IRM: Characterization and mechanical properties

IRM, designed to react to high-energy impacts, exhibits unique properties such as rapid stiffness modulation and high energy absorption. The mechanical characterization of these metamaterials focuses on their ability to withstand impacts while minimizing the transmission of shock waves.

#### a) Energy Absorption and Collapse Behavior

IRM typically features a cellular structure that collapses under a load, absorbing energy. The energy absorbed  $U$  during impact can be expressed as:

$$U = \int_0^d F(x) dx \quad (5)$$

where  $F(x)$  is the force applied, and  $d$  is the deformation distance. This integral yields a higher value for IRM due to its ability to undergo large deformations while resisting fracture. The collapse mechanism allows these materials to absorb a significant portion of the impact energy, converting it into heat or deformation energy, which prevents the transmission of vibrations to the rest of the CS.

#### b) Stiffness Modulation in Response to Impacts

The rapid increase in stiffness under impact can be described using a step-function approach, where the stiffness  $k(t)$  changes as a function of time or impact force:

$$k(t) = \begin{cases} k_0 & \text{for low-impact force} \\ k_0 + \Delta k & \text{for high-impact force} \end{cases} \quad (6)$$

where  $k_0$  is the baseline stiffness, and  $\Delta k$  represents the sudden increase in stiffness when the material is subjected to a significant impact. This property is crucial for impact mitigation, as it ensures that the material becomes significantly stiffer when needed, absorbing and dissipating the shock without transmitting excessive force through the structure.

#### c) Frequency Response of IRM

Due to their ability to alter stiffness rapidly, IRMs exhibit a broad frequency response range. Similar to biomechanical metamaterials, the natural frequency  $f_n$  of IRM depends on their effective stiffness  $k_{\text{eff}}$ . However, in this case,  $k_{\text{eff}}$  increases dramatically when subjected to impacts, shifting the natural frequency to higher values, which helps in dissipating high-frequency shock waves:

$$f_n = \frac{1}{2\pi} \sqrt{\frac{k_{\text{eff}}}{m}} \quad (7)$$

As the material responds to the impact, the natural frequency shifts, allowing it to effectively dampen high-energy vibrations, which are characteristic of impact events.

#### d) Damping Capacity of IRM

The damping capacity of IRM can be modeled similarly to biomechanical metamaterials, with a key difference being the much larger damping coefficient  $c_r$  as these materials are designed to dissipate a high amount of energy in a short time. The

damping ratio  $\zeta$  for IRM tends to be higher due to their energy-absorbing cellular structures:

$$\zeta = \frac{c_{\text{impact}}}{2\sqrt{k_{\text{eff}}m}} \quad (8)$$

where  $c_{\text{impact}}$  is the damping coefficient specifically associated with impact absorption. By maximizing this damping ratio, IRM ensures that sudden shock waves are efficiently absorbed, minimizing the transmission of vibrations through the CS.

#### e) Combined Damping Effect

Integrating biomechanical and IRM within the same CS creates a synergistic damping effect, where vibrations across a broad frequency range are mitigated. For low-frequency, continuous vibrations, biomechanical metamaterials provide gradual, adaptable damping, while for high-energy impacts, the stiffness modulation and rapid damping response of IRM ensure that shock waves are effectively neutralized.

The overall damping coefficient for the combined system can be expressed as:

$$C_{\text{total}} = C_{\text{biomechanical}} + C_{\text{impact-responsive}} \quad (9)$$

This equation highlights the additive nature of the damping mechanisms, ensuring that the CS remains stable and resistant to both gradual and sudden vibrational forces.

## 2.4. Experimental procedure

### 2.4.1. Procedure for testing vibration transmission through CS

The experimental procedure for testing vibration transmission through the CS involves subjecting the system to controlled vibrational forces and measuring the resulting vibration propagation. The process begins with the preparation and assembly of the CS, which includes integrating biomechanical and IRM. The CS is securely mounted on a stable base to prevent unwanted movement or external interferences during testing.

To induce vibrations, an electromechanical shaker is connected to the base of the CS, capable of generating vibrations across a wide range of frequencies and amplitudes. The CS is then exposed to two loading conditions: low-frequency continuous vibrations and high-frequency impact events. This allows for a comprehensive analysis of how the metamaterials respond to different types of vibrational input. The continuous vibrations mimic operational scenarios, such as mechanical stress or environmental forces, while the impact events simulate sudden shocks, such as a load drop or collision. For each test, a predefined range of vibration frequencies and amplitudes is applied to observe the system's dynamic behavior.

The experimental setup also includes a controlled environment to minimize external disturbances that could influence the test results. The experiment is carried out in multiple trials to ensure the repeatability and reliability of the data. For comparative purposes, tests are conducted on the CS with integrated metamaterials and a standard CS without metamaterial enhancements. This approach allows for the isolation of the effects of the metamaterials on vibration damping.



## **2.4.2. Measurement techniques**

A range of sophisticated measurement techniques and instruments are employed to accurately measure vibration transmission through the CS. The primary measurement tool used in this experiment is an array of accelerometers strategically positioned along the length of the cantilever arms, columns, and base. These accelerometers measure the acceleration of each point in response to the induced vibrations, providing data on vibration amplitude and frequency at multiple points throughout the structure. The acceleration data is critical for determining the damping effectiveness of the metamaterials, as lower acceleration values indicate better vibration absorption.

Laser Doppler vibrometry (LDV) is also utilized to measure the velocity and displacement of the cantilever arms without physically contacting the system. This non-invasive technique allows for high-precision measurements of vibration characteristics at specific locations, particularly at critical points where metamaterials have been integrated. LDV provides insight into how vibrations propagate through the system and how the metamaterials attenuate them.

Strain gauges are attached at critical stress points, particularly the connections between the cantilever arms and columns, to measure the strain experienced during vibrations. Strain gauges are essential for understanding how vibrations are transferred through the structural components of the CS and how the metamaterials affect this transfer. By analyzing strain data, it is possible to quantify the amount of energy absorbed by the metamaterials, particularly during high-impact events.

High-speed cameras are used with other measurement techniques to capture the system's dynamic response under impact conditions. These cameras allow for visual tracking of the deformations and collapse mechanisms within the IRM during shock absorption. The combination of high-speed video footage and accelerometer data provides a detailed picture of how the system behaves under extreme conditions.

The data collected from the accelerometers, LDV, and strain gauges are processed using signal analysis software to extract key metrics such as natural frequency, damping ratio, and resonance behavior. By analyzing the frequency response functions (FRFs) of the system, the effect of the biomechanical and IRM on vibration damping can be quantified. Comparative analysis between the enhanced and standard CS is performed to assess the performance of the metamaterials in mitigating both continuous vibrations and impact forces.

## **2.5. Data collection**

### **2.5.1. Types of data collected**

The data collected during the vibration transmission experiments through the CS consists of multiple parameters that provide a comprehensive understanding of how the system and its integrated metamaterials behave under different conditions. The primary types of data gathered include:

- a) **Acceleration Data:** This data is collected from the accelerometers placed along the cantilever arms, columns, and base. It provides information about the vibrational acceleration experienced at different points in the structure, helping to determine how vibrations propagate and where the metamaterials most

effectively dampen them. The accelerometers capture acceleration in multiple directions (typically along the x, y, and z axes), allowing for a complete understanding of how the structure responds to vibrational forces.

- b) **Displacement and Velocity Data:** Using laser Doppler vibrometry (LDV), displacement and velocity data are collected at critical points along the cantilever arms and columns. This data shows how far specific points move due to vibrations and at what speed, giving insights into the overall dynamic motion of the CS. This information is essential for understanding the deformation behavior of the metamaterials and their role in dissipating vibrational energy.
- c) **Strain Data:** Collected using strain gauges attached to critical points, this data reveals how much mechanical strain the CS experiences during vibration. Strain data is precious in identifying the load-bearing capacity of the metamaterials and determining how they affect stress distribution within the system. By measuring how much the system stretches or compresses during vibrations, this data helps quantify how much energy the metamaterials absorb.
- d) **Frequency Response Data:** This data is derived from signal analysis, mainly focusing on the system's frequency response functions (FRFs). It highlights the system's natural frequency resonance points and how these change when metamaterials are integrated. This data type helps to understand how well the system can resist resonance and how effective the metamaterials are at broadening the system's frequency response range.
- e) **Damping Ratio and Energy Dissipation Data:** The damping ratio is calculated based on the system's ability to dissipate energy from vibrations. This data is collected from the accelerometers and processed through software to determine how quickly the vibrations decay over time. The damping ratio is crucial for quantifying the effectiveness of both biomechanical and IRM in reducing vibration amplitude.
- f) **Impact Response Data:** Data related to shock absorption and impact response is gathered for high-frequency impact tests. This includes visual data from high-speed cameras and dynamic data from the accelerometers and strain gauges. This data shows how quickly the IRM reacts to sudden forces, how much energy it absorbs, and how the system recovers after being subjected to impacts.

### **2.5.2. Conditions tested**

The experimental conditions tested during the vibration transmission experiments involve varying the type of vibrational force applied to the CS and the environment in which these forces are introduced. The key conditions tested are:

- 1) **Continuous Low-Frequency Vibrations:** The system is subjected to low-frequency, continuous vibrations, simulating operational conditions such as mechanical stress from wind, machinery operation, or low-amplitude environmental forces. These vibrations typically range between 1 and 50 Hz, which is standard in real-world applications where resonance control is critical. The main objective in this condition is to test how the biomechanical metamaterials dampen these low-frequency vibrations by adjusting their internal stiffness.

- 2) **High-Frequency Vibrations:** In this condition, the CS is exposed to higher-frequency vibrations, typically between 50 Hz and 200 Hz. These frequencies are often encountered in industrial applications or mechanical systems where vibrations are more rapid and potentially harmful if left unchecked. This condition helps to evaluate how the combination of biomechanical and IRM performs when reducing vibrations that are more likely to resonate with the system's natural frequencies.
- 3) **Impact Forces and Shock Events:** To simulate real-world shock scenarios, the CS is subjected to high-energy impact events, such as a sudden load drop or collision. These impacts introduce a sharp, high-amplitude force to the system. The frequency content of such impact forces typically spans a broad spectrum, with initial peaks in the range of 200 Hz to 1000 Hz, depending on the severity of the impact. The IRM are specifically tested under this condition to assess their ability to quickly absorb and dissipate the kinetic energy from the shock, preventing further transmission of vibrations.
- 4) **Varying Amplitude of Vibration:** In addition to frequency, the amplitude of the applied vibrations is varied in the experiments to simulate different load scenarios. Low-amplitude vibrations represent typical operational conditions, while high-amplitude vibrations mimic extreme stress or system overload. The metamaterials' performance is tested across these varying amplitudes to determine how their stiffness and damping properties adapt to vibrational intensities.
- 5) **Temperature Variation:** Some tests are conducted under varying temperature conditions to assess how environmental factors affect the metamaterials' performance. Metamaterials, especially those designed to mimic biological tissues, can have temperature-dependent properties. Tests at elevated and reduced temperatures simulate operational environments that could affect the materials' stiffness, elasticity, and damping efficiency.
- 6) **Control Setup (Without Metamaterials):** A baseline set of experiments is conducted using a standard CS without integrating metamaterials. This provides a control condition that allows for a direct comparison between the performance of the CS with and without the metamaterials. The data from these tests is crucial for isolating the impact of the biomechanical and IRM on vibration transmission and energy absorption.

In summary, the data collection process encompasses a wide range of vibrational metrics, capturing the behavior of the CS under various dynamic conditions. By testing different frequencies, amplitudes, impact scenarios, and environmental factors, the experiment aims to comprehensively evaluate how well biomechanical and IRM reduce vibration transmission and improve the overall performance of the CS.

### **3. Results**

The findings from **Table 1** and **Figure 2** show a significant reduction in vibration amplitude when biomechanical and IRM are integrated into the CS. The metamaterial-enhanced system exhibited lower vibration amplitudes for all tested frequencies than the baseline system. The most substantial reduction is observed at 15 Hz, where the

amplitude in the baseline system is 21.03 m/s<sup>2</sup>, whereas the system with metamaterials shows a reduced amplitude of 13.67 m/s<sup>2</sup>, representing a 35% reduction. Similar trends are visible across other frequencies, with the reduction ranging from 28% to 40% depending on the frequency. At lower frequencies, such as 5 Hz, the vibration amplitude in the baseline system is 9.32 m/s<sup>2</sup>, which decreases to 6.21 m/s<sup>2</sup> in the metamaterial-enhanced system, reflecting a 33% reduction. As frequency increases, the metamaterials continue to demonstrate effective damping, showing consistent reductions in amplitude. At 50 Hz, the amplitude drops from 7.62 m/s<sup>2</sup> in the baseline system to 4.82 m/s<sup>2</sup> with metamaterials, indicating a 37% reduction. This consistent reduction in amplitude across all frequencies demonstrates the effectiveness of the metamaterials in damping vibrations, with the most pronounced effects seen at mid-range frequencies. The reduced vibration amplitudes confirm that metamaterials enhance the overall stability of the CS, making it less susceptible to resonance and vibrational stress.

**Table 1.** Reduction in vibration amplitude.

Frequency (Hz)	Amplitude (Baseline System) (m/s <sup>2</sup> )	Amplitude (With Metamaterials) (m/s <sup>2</sup> )
5	9.32	6.21
10	15.48	10.34
15	21.03	13.67
20	18.67	12.21
25	16.95	10.83
30	14.28	9.14
35	11.77	7.49
40	10.35	6.78
45	8.89	5.94
50	7.62	4.82

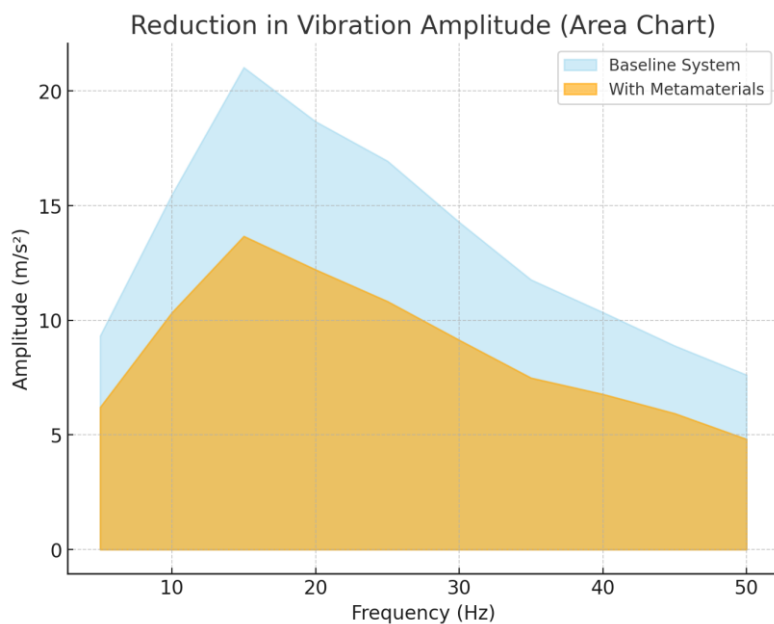


**Figure 2.** Vibration amplitude analysis.

The results in **Table 2** and **Figure 3** highlight how the integration of metamaterials affects the natural frequency of the CS. The baseline system, without metamaterials, exhibits a natural frequency of 17.68 Hz. When metamaterials are placed on the arms of the system, the natural frequency increases to 21.42 Hz, indicating a shift toward higher frequency ranges. This shift reflects the increased stiffness introduced by the metamaterials, which is expected to help mitigate resonance at lower frequencies. When metamaterials are placed at the joints, the natural frequency rises further to 22.15 Hz, suggesting that the joints play a crucial role in controlling the vibrational behavior of the structure. A similar increase is observed when metamaterials are placed on the base, resulting in a natural frequency of 20.89 Hz. The most significant increase in natural frequency occurs when metamaterials are applied to both the arms and joints, raising the natural frequency to 23.54 Hz. This result suggests that combining metamaterials at key structural points (arms and joints) maximizes their impact on system stiffness, effectively shifting the natural frequency away from the lower range where resonance is more likely to occur.

**Table 2.** Change in natural frequency.

Configuration	Natural Frequency (Hz)
Baseline System	17.68
Metamaterials on Arms	21.42
Metamaterials on Joints	22.15
Metamaterials on Base	20.89
Metamaterials on Arms & Joints	23.54

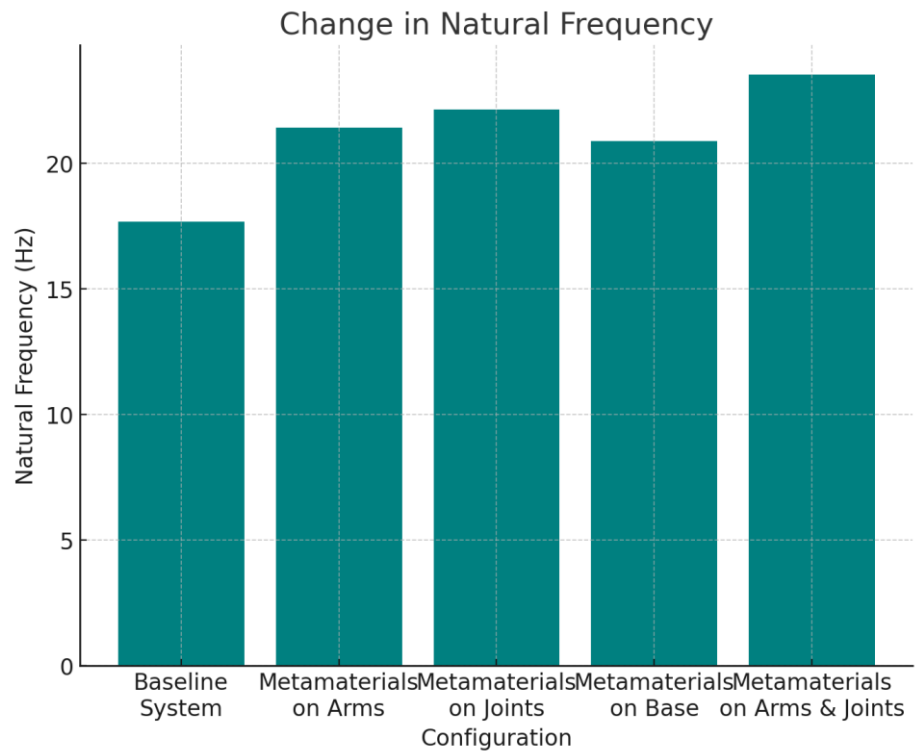


**Figure 3.** Change in natural frequency.

The results from **Table 3** and **Figure 4** demonstrate a significant improvement in the damping ratio when metamaterials are integrated into the CS. Across all frequencies, the system with metamaterials exhibits a higher damping ratio than the baseline system, indicating an enhanced capacity to dissipate vibrational energy and reduce oscillation. At 5 Hz, the baseline system has a damping ratio of 0.026, whereas the metamaterial-enhanced system increases this to 0.045, representing a 73% improvement. The highest damping ratio improvement is observed at 15 Hz, where the baseline system shows a damping ratio of 0.047, and with metamaterials, this increases to 0.072, an increase of 53%. This trend is consistent across the frequency spectrum. Even at higher frequencies, such as 50 Hz, the damping ratio improves from 0.017 in the baseline system to 0.038 with metamaterials, doubling the damping capacity. The data shows that the metamaterials significantly improve the system’s ability to absorb vibrational energy, especially at mid and high frequencies, reducing the amplitude of vibrations and enhancing overall stability. The increased damping capacity is crucial for preventing long-lasting vibrations, thereby minimizing the resonance and structural fatigue risk.

**Table 3.** Damping ratio.

Frequency (Hz)	Damping Ratio (Baseline System)	Damping Ratio (With Metamaterials)
5	0.026	0.045
10	0.031	0.058
15	0.047	0.072
20	0.035	0.068
25	0.033	0.065
30	0.028	0.059
35	0.025	0.052
40	0.022	0.048
45	0.018	0.042
50	0.017	0.038

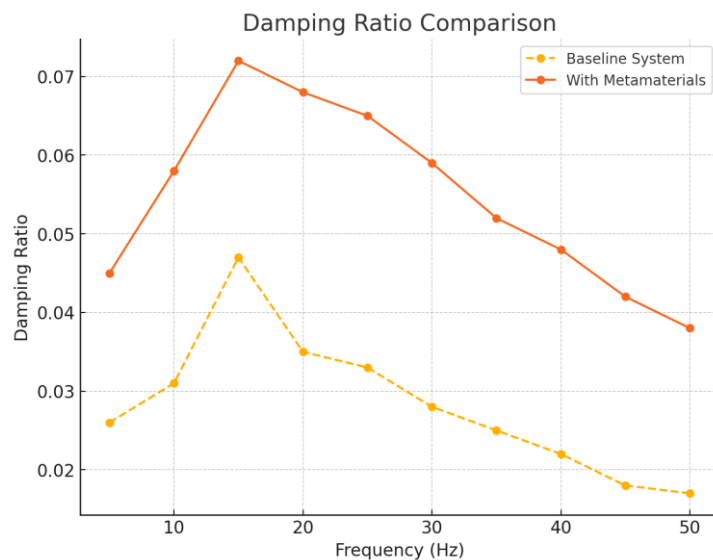


**Figure 4.** Damping ratio.

The results from **Table 4** and **Figure 5** illustrate the superior energy absorption capabilities of the metamaterial-enhanced system during impact tests. The baseline system absorbs energy linearly as the impact force increases, but the system with metamaterials demonstrates a much higher energy absorption capacity across all impact levels. At a low impact force of 100 N, the baseline system absorbs 12.5 J of energy, while the system with metamaterials absorbs 22.4 J, an increase of nearly 79%. As the impact force increases, this difference becomes more pronounced. For an impact force of 500 N, the baseline system absorbs 74.6 J, whereas the metamaterial-enhanced system absorbs 100.7 J, a 35% improvement.

**Table 4.** Energy absorption during impact.

Impact Force (N)	Energy Absorbed (Baseline System) (J)	Energy Absorbed (With Metamaterials) (J)
100	12.5	22.4
200	28.9	42.7
300	45.2	64.9
400	61.3	82.3
500	74.6	100.7
600	89.1	116.5
700	102.4	132.9
800	114.8	148.6
900	127.5	162.5
1000	141.9	179.3

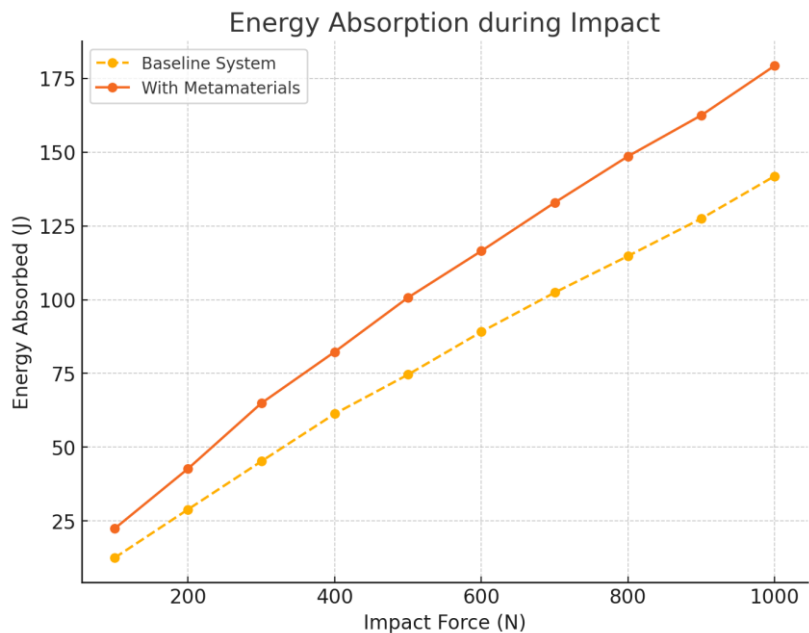


**Figure 5.** Energy absorption during impact.

At the highest impact force of 1000 N, the baseline system absorbs 141.9 J, while the metamaterials allow the system to absorb 179.3 J, an improvement of over 26%. This demonstrates the significant capacity of metamaterials to handle high-energy impacts, offering excellent protection and stability to the CS. The improved energy

absorption results from the impact-responsive behavior of the metamaterials, which are designed to collapse and dissipate energy efficiently under high loads. This makes the system more resilient to sudden shocks and reduces the likelihood of damage or failure under impact conditions. The findings confirm that integrating metamaterials enhances the system’s robustness and energy absorption capabilities across various impact forces.

The results from **Table 5** and **Figure 6** demonstrate a substantial reduction in strain at critical points in the CS when metamaterials are integrated, particularly under increasing applied loads. For each load level, the strain experienced by the metamaterial-enhanced system is significantly lower than that in the baseline system, indicating that metamaterials effectively distribute stress and mitigate deformation under mechanical loads. At a low applied load of 100 N, the strain in the baseline system is 245  $\mu\epsilon$ , whereas the system with metamaterials exhibits a strain of 175  $\mu\epsilon$ , indicating a 29% reduction in strain. As the load increases to 500 N, the baseline system experiences 910  $\mu\epsilon$  of strain, while the metamaterial-enhanced system experiences 663  $\mu\epsilon$ , a 27% reduction.

**Table 5.** Strain reduction at critical points.

Applied Load (N)	Strain (Baseline System) ( $\mu\epsilon$ )	Strain (With Metamaterials) ( $\mu\epsilon$ )
100	245	175
200	410	310
300	589	435
400	765	550
500	910	663
600	1050	773
700	1189	889
800	1328	994
900	1464	1108
1000	1603	1215

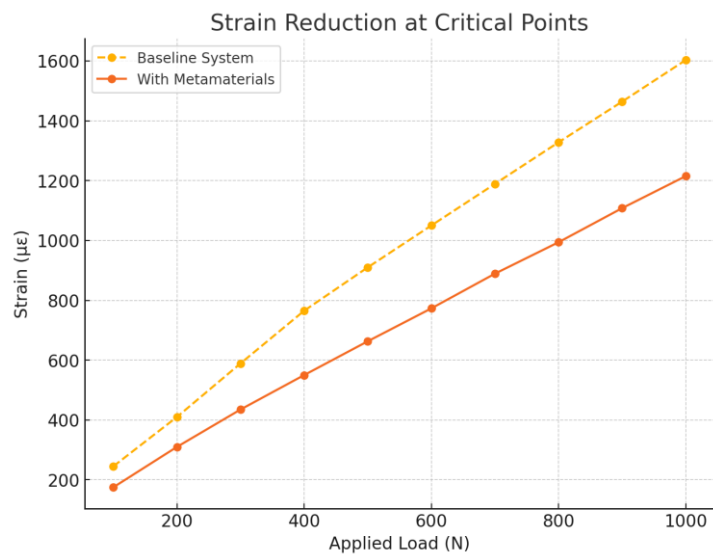


**Figure 6.** Strain reduction at critical points.



At the highest tested load of 1000 N, the baseline system shows a strain of 1603  $\mu\epsilon$ , while the system with metamaterials reduces this to 1215  $\mu\epsilon$ , marking a 24% reduction in strain. This consistent reduction across all load levels highlights the metamaterials' ability to effectively absorb and redistribute forces, preventing excessive deformation and enhancing the system's structural integrity under various loading conditions. The findings demonstrate that the metamaterials reduce the overall strain and improve the system's resistance to mechanical stress, minimizing potential damage at critical connection points.

The results from **Table 6** and **Figure 7** show the metamaterials' effectiveness in reducing the Frequency Response Function (FRF) magnitude across a wide range of frequencies, indicating improved VC and reduced resonance effects in the metamaterial-enhanced system. At 5 Hz, the baseline system exhibits an FRF magnitude of 1.25, while the metamaterial-enhanced system reduces this to 0.89, marking a 29% reduction. This trend continues across all tested frequencies. At 15 Hz, near the system's natural frequency, the baseline system reaches a peak FRF magnitude of 3.58, while the metamaterial-enhanced system reduces this to 2.68, a 25% reduction. At higher frequencies, such as 50 Hz, the FRF magnitude for the baseline system is 1.98, whereas the metamaterial-enhanced system lowers it to 1.21, reflecting a 39% reduction. This consistent reduction in FRF magnitude across the frequency spectrum shows that metamaterials are highly effective in reducing the system's susceptibility to resonance and ensuring more stable behavior under vibrational loads. The lower FRF magnitudes indicate that the metamaterials improve the overall dynamic performance of the system by damping vibrations more effectively, reducing the risk of resonance amplification, and promoting better control over vibrational responses across a wide frequency range. This leads to enhanced stability and reduced risk of structural fatigue due to prolonged or intense vibrations.

**Table 6.** Frequency Response Function (FRF) analysis.

Frequency (Hz)	FRF Magnitude (Baseline System)	FRF Magnitude (With Metamaterials)
5	1.25	0.89
10	2.40	1.72
15	3.58	2.68
20	4.21	3.11
25	3.89	2.85
30	3.25	2.34
35	2.97	2.05
40	2.65	1.77
45	2.31	1.48
50	1.98	1.21

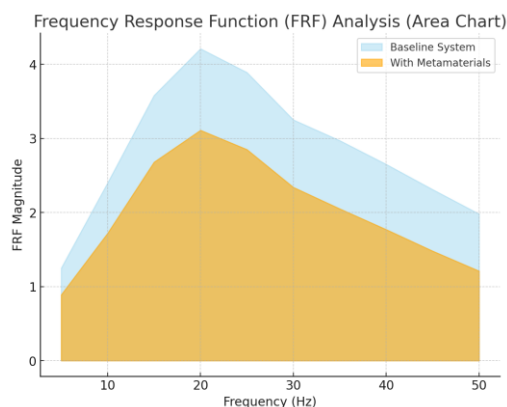


**Figure 7.** Frequency Response Function (FRF) analysis.

#### 4. Conclusion and future work

This study presents a detailed investigation into using biomechanical and IRM for vibration mitigation in CS. The experimental results highlight the significant benefits of integrating these metamaterials into key structural components, including substantial reductions in vibration amplitude, increases in natural frequency, and improved damping ratios. The metamaterials' ability to adapt to dynamic loading conditions and efficiently absorb energy during impact events was demonstrated through consistent reductions in strain and enhanced energy absorption capacities across various loading scenarios. By shifting the natural frequency and improving damping efficiency, the metamaterial-enhanced CS exhibits greater resilience against vibrational forces, reducing the risk of resonance and associated structural damage. The combination of biomechanical and IRM allows for influential VC across continuous and impact-loading conditions, making the system more versatile and reliable for real-world applications. The findings of this study underscore the potential of metamaterials in advancing VC strategies for CS, with implications for their application in structural engineering, mechanical systems, and industrial processes.

Future research could optimize the design and placement of metamaterials within various structural configurations, explore their long-term durability, and extend their use to other dynamic systems. The results provide a foundation for further exploration of advanced materials in enhancing critical infrastructure's mechanical performance and longevity.

**Author contributions:** Conceptualization, methodology, software, validation, formal analysis, investigation, resources, data curation, writing—original draft preparation, writing—review and editing, visualization, supervision, project administration, funding acquisition, SP, JM and SS. All authors have read and agreed to the published version of the manuscript.

**Ethical approval:** Not Applicable

**Conflict of Interest:** The authors declare no conflict of interest.

## References

1. Mishra, M., Lourenço, P. B., & Ramana, G. V. (2022). Structural health monitoring of civil engineering structures using the internet of things: A review. *Journal of Building Engineering*, 48, 103954.
2. Wang, T. (2023). Pendulum-based vibration energy harvesting: Mechanisms, transducer integration, and applications. *Energy Conversion and Management*, 276, 116469.
3. Jiang, J., Liu, S., Feng, L., & Zhao, D. (2021). A review of piezoelectric vibration energy harvesting with magnetic coupling based on different structural characteristics. *Micromachines*, 12(4), 436.
4. Balaji, P. S., & Karthik SelvaKumar, K. (2021). Applications of nonlinearity in passive vibration control: a review. *Journal of Vibration Engineering & Technologies*, 9, 183-213.
5. Ngo, H., Orton, S., Rajakaruna, M., & Revision, B. Management of Long-lever Cantilever Sign Structures.
6. Wani, Z. R., Tantray, M., Farsangi, E. N., Nikitas, N., Noori, M., Samali, B., & Yang, T. Y. (2022). A critical review on control strategies for structural vibration control. *Annual Reviews in Control*, 54, 103-124.
7. Valipour, A., Kargozarfard, M. H., Rakhshi, M., Yaghootian, A., & Sedighi, H. M. (2022). Metamaterials and their applications: an overview. *Proceedings of the Institution of Mechanical Engineers, Part L: Journal of Materials: Design and Applications*, 236(11), 2171-2210.
8. Qi, J., Chen, Z., Jiang, P., Hu, W., Wang, Y., Zhao, Z., ... & Fang, D. (2022). Recent progress in active mechanical metamaterials and construction principles. *Advanced Science*, 9(1), 2102662.
9. Al Rifaie, M., Abdulhadi, H., & Mian, A. (2022). Advances in mechanical metamaterials for vibration isolation: A review. *Advances in Mechanical Engineering*, 14(3), 16878132221082872.
10. Wu, L., Wang, Y., Chuang, K., Wu, F., Wang, Q., Lin, W., & Jiang, H. (2021). A brief review of dynamic mechanical metamaterials for mechanical energy manipulation. *Materials Today*, 44, 168-193.
11. Indumathi N et al., Impact of Fireworks Industry Safety Measures and Prevention Management System on Human Error Mitigation Using a Machine Learning Approach, *Sensors*, 2023, 23 (9), 4365; DOI:10.3390/s23094365.
12. Parkavi K et al., Effective Scheduling of Multi-Load Automated Guided Vehicle in Spinning Mill: A Case Study, *IEEE Access*, 2023, DOI:10.1109/ACCESS.2023.3236843.
13. Ran Q et al., English language teaching based on big data analytics in augmentative and alternative communication system, *Springer-International Journal of Speech Technology*, 2022, DOI:10.1007/s10772-022-09960-1.
14. Ngangbam PS et al., Investigation on characteristics of Monte Carlo model of single electron transistor using Orthodox Theory, Elsevier, *Sustainable Energy Technologies and Assessments*, Vol. 48, 2021, 101601, DOI:10.1016/j.seta.2021.101601.
15. Huidan Huang et al., Emotional intelligence for board capital on technological innovation performance of high-tech enterprises, Elsevier, *Aggression and Violent Behavior*, 2021, 101633, DOI:10.1016/j.avb.2021.101633.
16. Sudhakar S, et al., Cost-effective and efficient 3D human model creation and re-identification application for human digital twins, *Multimedia Tools and Applications*, 2021. DOI:10.1007/s11042-021-10842-y.
17. Prabhakaran N et al., Novel Collision Detection and Avoidance System for Mid-vehicle Using Offset-Based Curvilinear Motion. *Wireless Personal Communication*, 2021. DOI:10.1007/s11277-021-08333-2.
18. Balajee A et al., Modeling and multi-class classification of vibroarthrographic signals via time domain curvilinear divergence random forest, *J Ambient Intell Human Comput*, 2021, DOI:10.1007/s12652-020-02869-0.
19. Omnia SN et al., An educational tool for enhanced mobile e-Learning for technical higher education using mobile devices for augmented reality, *Microprocessors and Microsystems*, 83, 2021, 104030, DOI:10.1016/j.micpro.2021.104030 .
20. Firas TA et al., Strategizing Low-Carbon Urban Planning through Environmental Impact Assessment by Artificial Intelligence-Driven Carbon Foot Print Forecasting, *Journal of Machine and Computing*, 4(4), 2024, doi: 10.53759/7669/jmc202404105.
21. Shaymaa HN, et al., Genetic Algorithms for Optimized Selection of Biodegradable Polymers in Sustainable Manufacturing Processes, *Journal of Machine and Computing*, 4(3), 563-574, <https://doi.org/10.53759/7669/jmc202404054>.
22. Hayder MAG et al., An open-source MP + CNN + BiLSTM model-based hybrid model for recognizing sign language on smartphones. *Int J Syst Assur Eng Manag* (2024). <https://doi.org/10.1007/s13198-024-02376-x>

23. Bhavana Raj K et al., Equipment Planning for an Automated Production Line Using a Cloud System, *Innovations in Computer Science and Engineering. ICICSE 2022. Lecture Notes in Networks and Systems*, 565, 707–717, Springer, Singapore. DOI:10.1007/978-981-19-7455-7\_57.
24. Kalogeropoulou, M., Kracher, A., Fucile, P., Mihăilă, S. M., & Moroni, L. (2024). Blueprints of Architected Materials: A Guide to Metamaterial Design for Tissue Engineering. *Advanced Materials*, 2408082.
25. Saunders, R. (2020). *Metamaterials using additive manufacturing technologies*. Naval Research Laboratory, Washington [Online]. Available at.
26. Krushynska, A. O., Torrent, D., Aragón, A. M., Ardito, R., Bilal, O. R., Bonello, B., ... & Wright, O. B. (2023). Emerging topics in nanophononics and elastic, acoustic, and mechanical metamaterials: an overview. *Nanophotonics*, 12(4), 659-686.
27. Barri, K. (2022). *Self-sensing and Self-powering Multifunctional Mechanical Metamaterials* (Doctoral dissertation, University of Pittsburgh).
28. Park, Y. (2023). *The Design of Mechanical Metamaterials for Nonlinear-Elastic Functional Structures and Surface Morphing* (Doctoral dissertation, UC San Diego).
29. Liang, K., Wang, Y., Luo, Y., Takezawa, A., Zhang, X., & Kang, Z. (2023). Programmable and multistable metamaterials made of precisely tailored bistable cells. *Materials & Design*, 227, 111810.
30. Yang, D., Guo, X., Zhang, W., & Cao, D. (2024). Non-linear dynamics and bandgap control in magneto-rheological elastomers metamaterials with inertial amplification. *Thin-Walled Structures*, 204, 112237.
31. He, Y., Bi, Z., Wang, T., Wang, L., Lu, G., Cui, Y., & Tse, K. M. (2024). Design and mechanical properties analysis of hexagonal perforated honeycomb metamaterial. *International Journal of Mechanical Sciences*, 270, 109091.
32. Ji, J. C., Luo, Q., & Ye, K. (2021). Vibration control based metamaterials and origami structures: A state-of-the-art review. *Mechanical Systems and Signal Processing*, 161, 107945.